Evaluation of the observed damage and rehabilitation study of two underground R/C biological treatment tanks

G. Gr. Penelis[1], Gr. G. Penelis[1], A.G. Sextos[1]

[1] *Aristotle University of Thessaloniki, Greece*

Abstract

This paper focuses on the evaluation of the damage observed on two adjacent reinforced concrete tanks, part of the Biological Treatment complex of Thessaloniki, Greece, after their abrupt evacuation that occurred while the water table level was relatively high compared to the initial design assumptions. These tanks exhibited large vertical displacements (up to 0.90m at certain locations) and extensive radial cracks at their bottom. Based on the observations made right after the damage, a detailed assessment was performed aiming at: a) obtaining an insight on the cause and the mechanisms of failure b) investigate the rehabilitation potential as compared to the complete reconstruction cost of the tanks, and c) propose the rehabilitation scheme towards the functionality restoration of the tanks. Along with detailed design and assessment calculations based on the existing evidence and damage patterns observed, a set of refined non-linear finite element analyses was performed for all successive stages of water evacuation. The implemented static nonlinear analysis approach accounts for plastic deformations of both reinforced concrete body and soil, gradually increasing uplift load as well as varying gapping properties at the soil-tank interface. It is concluded that the plastic behavior of the reinforced concrete tank substantially affected the force redistribution during the evacuation process, resulting to an actual, self- balanced condition that was significantly different as compared to the deformation predicted on the assumptions of linear elastic behaviour of the system.

STATEMENT OF THE PROBLEM

The paper is a brief report of the damage assessment and retrofit proposal following the damage and deformation observed at two of the four underground final consolidation tanks of the sewage biological treatment plant of Thessaloniki

The tanks consist of a perimeter wall with a depth t=0.45m, a bottom slab with a depth t=0.38m (excluding the area adjacent to the perimeter wall where it increases to t=0.50m) and an internal central tower. The tanks have a diameter of 54,00m and a depth varying from 4.84m at the perimeter to 6.80m at the center (outer perimeter of the central tower, as seen in Fig.1,3). They have been constructed with grade C20/25 concrete and steel reinforcement S500s.

During Electro-Mechanical (E&M) works those tanks were evacuated without prior checking of the water table level, the latter being in fact significantly higher than that assumed during design (i.e 3,60m to 3,80m instead of 2.00m respectively). This condition resulted into deformation of the bottom slab equal to 30cm and 90 cm in the two tanks as well as cracking of the top surface of the bottom slab in a hairline random pattern which was transformed into radial cracks along the perimeter. Moreover, vertical cracks developed along the first meter of the outer perimeter wall and tilting of the center tower was observed

Following the above damage, the two tanks were refilled while monitoring the level and grade of restoration of the deformations of the bottom slab. The latter were indeed reduced to only 5-15cm and the central tower was restored to its vertical position.

Following these events an extensive restoration design procedure commenced utilizing the contractors design team (Themeliodomi SA), the technical consultants of the owner (MWH UK ltd) and the authors as the external experts. The main task of all the design efforts was the determination of the stress and strain level at the bottom surface of the foundation slab, which was not visible. In particular it was deemed necessary to assess whether crushing of concrete had taken place due to compression. Both the analytical calculations utilizing the observed data (deformations and crack width) and the purely numerical approach demonstrate that the compression zone of the slab did not reach its capacity due to flexural strain. As a result, the tanks could be restored and reconstruction was finally avoided.

EVALUATION OF THE OBSERVED FOUNDATION DAMAGE

The evaluation of the observed damage of the foundation bottom slab and the perimeter wall was performed in order to analytically simulate the mechanisms developed after the exceedence of the design forces and to assess the condition of the non-visible parts of the tanks. To evaluate the damage the following data had to be taken into account:

(a) Damage pattern of the empty tank regarding cracking, concrete crushing at the compression zones due to flexure, initial deformations after evacuation, and serviceability of the tanks,
(b) Condition of the tanks after their refill in terms of remaining cracks, concrete crushing at the compression zones due to flexure, residual deformations and serviceability of the tanks,
(c) Evaluation of the stress state of the tanks due to the increased water uplift.

DAMAGE PATTERN OF THE EMPTY TANKS

The damage pattern of the empty tanks and the interpretation of the failure mechanisms is presented in the same manner as the one of the refilled tanks in order to demonstrate the evolution of the damage and deformations.

(a) Cracking pattern

The cracking pattern of the tanks can be categorized in three main groups on the basis of their orientation, (i.e. ring, radial and hairline random cracks)

(i) Ring cracks at the intermediate zone of the bottom slab between the center tower and the perimeter wall. Those cracks in relation to the stress state of the elastic analysis performed, can be attributed to the yielding of the radially placed reinforcement at the top of the slab, due to high bending moments.
(ii) Radial cracks originating from the outer third of the bottom slab and extending to the perimeter vertical wall up to 1,00m height. Relating those to the elastic analysis , they can be attributed to the yielding of the circular reinforcement, placed at the whole depth of the bottom slab, due to high tensile forces tangent to the perimeter.
(iii) Random hairline cracks at the top surface of the bottom slab, which resemble initial shrinkage cracks intensified by the increased stresses.

The first and second groups of cracks are at distances of 20-25cm at the critical zones and have a width of 0,50mm to 1,00mm. Those observations are in good agreement with the analytical calculations.

(b) Concrete crushing at the compression zones

The expected areas of concrete crushing, as defined by the analytical simulations, can be summarized as follows:

(i) The interior circular surface of the perimeter wall adjacent to the connection to the bottom slab, a zone that no damage was observed
(ii) The top surface of the bottom slab, adjacent to the connection to the perimeter wall, a zone that also exhibited no damage
(iii) The bottom surface of the slab in the zone ranging from a radius of 12,50m to 20.00m. In this zone the higher bending moments are developed with a vector tangent to the perimeter which combined with the radial membrane stresses causes radial compression. Since this zone is on the bottom surface of the foundation slab, which is not visible, only an analytical calculation is feasible.

This calculation is based on the elongation of the yielded reinforcement at the tension zones and the calculation of the curvature using the width of the cracks (Fig. 1,2). The total measured width of the cracks was calculated to correspond to an elongation of ε= 2,50-4,00‰ leading to the conclusion that the capacity of the compression zone was not reached. Indeed, for an elongation of 4,50‰ on the top surface and shrinkage of the concrete at the bottom surface equal to 3.50‰ (the maximum accepted by Eurocode 2), the available capacity of the compression zone is found equal to 1885KN.

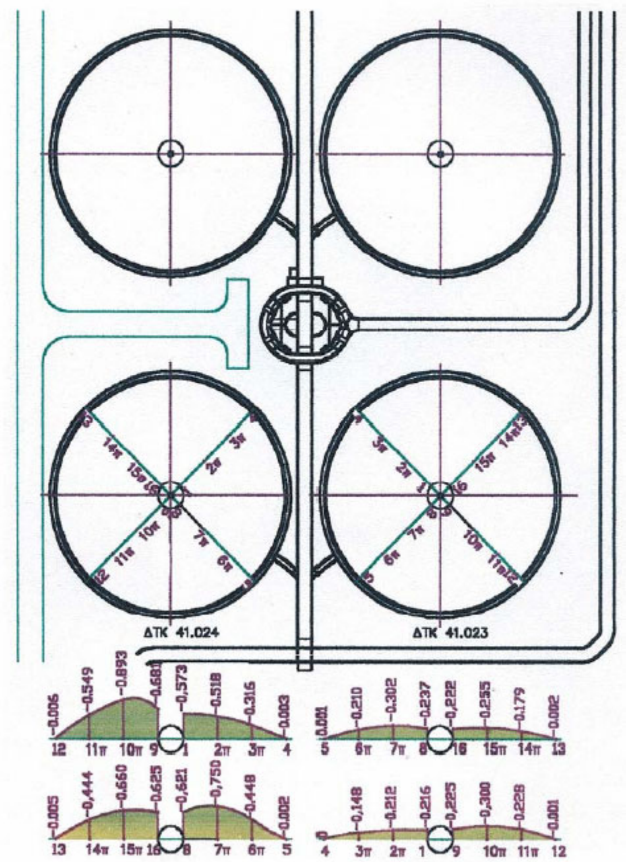

Fig. 1: Deformation of the foundation slab

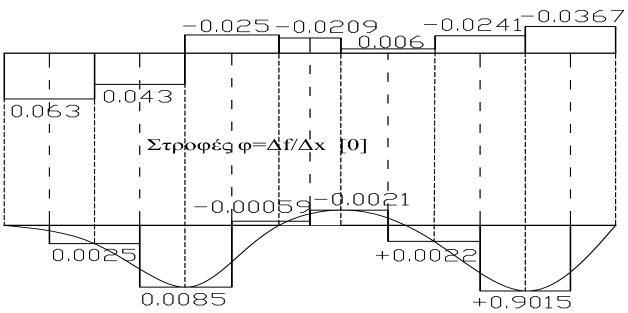

Fig.2: Calculated corresponding curvatures

The compression force therefore required to balance the yield force of the yielded reinforcement is approximately 450KN. which is much lower than the compressive capacity.
To summarise all the above, it is safe to analytically conclude that no crushing of concrete due to compression took place at any surface of the tanks, and only cracking due to yielding of the reinforcement took place. As stated previously this is a very critical point for the decisions made regaring the tank retrofit.

(c) Deformations following the evacuation of the tanks

As has been already mentioned, following the abrupt evacuation of the tanks, large deformations were observed. Those consisted of negligible vertical displacement of the perimeter walls (0-6mm) and a maximum bottom slab displacement of 0.89m and 0.30mm for the two tanks respectively) as seen in Fig.1. Moreover, uplift and tilting of the central tower of the order of 0.60m was observed with a 2% inclination for the case of the first tank and 0.23m without visible inclination for the second tank.
Utilizing the above observations, the following conclusions were derived:

- The tank did not move as a solid body due to the water uplift, meaning that its self weight and the developed frictional forces between the external surface of the perimeter RC wall and the soil balanced the uplift forces. This essentially lead to the development of an internal stress path.
- Although the observed maximum deformation of the bottom slab (i.e. 0.89m), may seem impressive, it corresponds to an elongation of the top surface due to flexure of 3,3‰, which is rather reasonable considering the large dimensions of the tank (Diameter D=54.00m)

(d) Serviceability

Following the uplift of the central part of the bottom slab of the tanks and their cracking, no water leakage was observed from the outside high water table to the inside of the empty tanks. This fact supports the estimation that neither crushing of the concrete took place at the compression zones, nor the elongation of the yielded reinforcement was large enough to significantly decrease the depth of these compression zones and facilitate, in that way leakage from the outside to the inner part of the tank.

DAMAGE PATTERN OF THE REFILLED TANKS

Following the refill of the tanks, the above observations were made:

(a) Cracking pattern

The crack width was significantly decreased, which was expected in connection to the decrease in the deformations, described in the following paragraph

(b) Deformations following the refill of the tanks

The remaining deformations were 5-13 cm in the first tank and 8-23cm in the second tank, while the central towers were practically restored to their vertical position.

(c) Serviceability

The leakage per day was measured at $40m^3$/24hours which is considered a low value. This was an expected value since the residual deformation of the reinforcement was calculated less than 0.8‰, corresponding to a crack width of less than 0.15mm

EVALUATION OF THE CONDITION PRIOR TO RETROFITTING

All the above observations regarding, damage, deformations and serviceability (mainly in terms of water permiability) lead to a set of conclusions which are summarized in the following paragraphs.

At first, it has to be noted that the tanks subjected to the initial design loads do not exhibit any deficiencies either at the ultimate or the serviceability limit states. As a result, it can be drawn that had the water table not risen from +2.00m to +3.80m there would not have been any problems and damage.

On the other hand, the tanks were subjected to an increased uplift, corresponding to water table level of +4.00m developing elastic stresses many times higher than the design ones. In other words, had the material behaved linearly elastic, the tanks would have failed. More specifically, the bottom slab and the connections to the perimeter wall would have severely failed and the outside water table would have violently filled the inside of the empty tanks. Since that did not take place, and taking into account that no crushing of concrete took place, it can be safely concluded that nonlinear behaviour was developed leading to the redistribution of the elastic stresses. This behaviour was simulated using nonlinear analysis of the tanks, the results of which are presented in the following section.

The most crucial conclusion though, is that the tanks presented only deformations due to yielding of reinforcement without even reaching high elongation values. This occurred despite the fact that the tanks were subjected to extremely high uplift forces. As a result, the large deformation of the bottom slab, measured as 0.89m is attributed to the dimensions of the tank and not to the elongation of the reinforcement which is as low as 4‰ compared to a limit value of 20‰. In confirmation of that, no leakage was observed from the outside water table towards the empty tanks.

The refilled tanks were almost completely restored regarding deformations while their leak was very low.

Based on the above, the proposed restoration scheme was restricted to retrofitting and strengthening of all the required areas of the tanks without any major reconstruction.

OVERVIEW OF THE MULTI-PHASE 3D INELASTIC ANALYSIS SCHEME

The analysis of the tank was performed with the use of the widely used commercial code ANSYS implementing a 3D FE model, consisting of 1200 shell type elements with 6 degrees of freedom per node. These elements were adopted due to their plastic deformation capabilities and were meshed adequately densely at the locations of abrupt stiffness or geometry change. The width of the elements was also varying from 0.38m to 0.50m in order to account for the increased bottom width at the vicinity of the perimeter walls. With the use of 850 Unii-axial (compression only) spring elements which were attached to the foundation (along the vertical axis) as well as around the perimeter walls, the soil flexibility was accounted for.

It is noted that the Winkler-type lateral soil pressure was considered based on their effectiveness comparison and calibration with shell elements in 2D problems again with the FE code ANSYS (Kappos and Sextos, 2001). Moreover, they were applied in radial coordinates using a specifically written APDL script, a description and an application of which can be found elsewhere (ANSYS, 2004 and Sextos, 2005) The properties of the soil springs are given in Table 2 based on Mylonakis et al (2003).

The loads applied were a) self weight b) lateral soil pressure (γ=19 kN/m^3, K_A=0.33) and the hydrostatic pressure. It is clear that the hydrostatic pressure (i.e. as both lateral pressure and uplift) is dependent on the relative level of the sewage inside the tank and the water level within the surrounding soil, hence as the tank is gradually evacuated it essentially varies with depth and time. For the assessment of the non-linear behaviour of the R/C tank members (i.e. bottom and walls) two alternative material laws were implemented. In particular the Drucker-Prager and the Von-Mises models (Bi-linear Isotropic Hardening) were used. It was found that the latter, was more effective and in representing the behaviour of reinforced concrete.

Having assumed a friction angle φ = 0, a cohesion $c = \dfrac{\sqrt{3}(3-\sin\phi)\cdot\sigma_y}{6\cos\phi}$ =0.86σ_y (given that φ=0) a flow angle ψ=0, and a second branch stiffness equal to 1 ‰ of the initial one, the non-linear analysis was performed and particular convergence criteria were set.

It is noted that as the sewage level inside the tank is diminished, the tank bottom is gradually yielding thus spreading the plasticity, whereas different regions of soil compression are activated leading to a time-dependent lateral soil resistance. As a result, the substantial non-linear behaviour is both material and geometrical attributed.

Another important aspect of the material non-linearity is the derivation of an equivalent failure surface that considers the tensile strength of the steel compared to the behaviour of concrete alone. In the following, the calculation of an equivalent section yielding stress is provided.

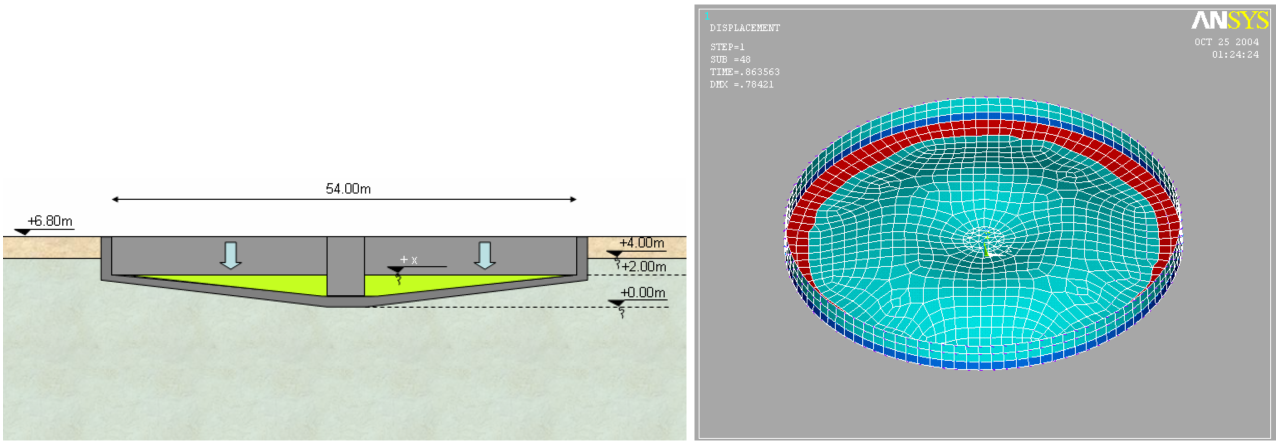

Fig.3: Overview of the geometrical properties of the problem and deformed shape of evacuated tank

Case 1: Pure bending without axial force (N=0):

For a section subjected to a bending moment M, the yielding stress σ_F can be calculated as follows, as a function of the section depth d, the reinforcement area A_s and the steel tensile strength f_{yd} (Fig. 4):

$$M = \overline{\sigma}_F \frac{d}{2}\frac{d}{2} = \overline{\sigma}_F \frac{d^2}{4}$$

$$M = A_s f_{yd} d$$

$$\overline{\sigma}_F = \frac{4A_s f_{yd}}{d} = 2\cdot\frac{2A_s f_{yd}}{d} \qquad (1)$$

Case 2: Pure tension without bending (M=0) (Fig. 5)

$$z_{\sigma\upsilon\nu} = 2A_s f_{yd}$$

$$z_{\sigma\upsilon\nu} = \overline{\sigma}_F d$$

$$\overline{\sigma}_F = \frac{2A_s f_{yd}}{d} = 1\cdot\frac{2A_s f_{yd}}{d} \qquad (2)$$

Case 3: Uniaxial Bending - Tension (e = M/N = 0.93) (Fig. 6)

With the assumption that the axial load is equal to:

$$\mathrm{N} = \overline{\sigma}_F \frac{d}{4}$$

$$M = \frac{3}{8}d \cdot \overline{\sigma}_F (\frac{d}{4} + \frac{3}{8}d) = \frac{3}{8}d^2 \overline{\sigma}_F (\frac{2}{8} + \frac{3}{8}) = \frac{3}{8}d^2 \overline{\sigma}_F \frac{5}{8}$$

=> e=M/N = 60/64d

e/d = 60/64

$$Z + D = \overline{\sigma}_F \frac{d}{4} = f_{yd} A_A - \sigma_e A_s$$

$$M = f_{yd} A_s \frac{d}{2} + \sigma_e A_s \frac{d}{2}$$

$$\overline{\sigma}_F = \frac{64}{46} \cdot \frac{2 A_s f_{yd}}{d} \qquad (3)$$

Case 4: Uniaxial Bending - Tension (e = M/N = 0.33) (Fig. 7)

$$\mathrm{N} = \overline{\sigma}_F \frac{4d}{8}$$

$$M = \frac{2}{8}d \cdot \overline{\sigma}_F (\frac{6}{8}d) = \frac{12}{64}d^2 \overline{\sigma}_F$$

=> e=M/N = 24/64d

e/d = 24/64

$$M = f_{yd} A_s \frac{d}{2} + \sigma_e A_s \frac{d}{2}$$

$$\overline{\sigma}_F = \frac{64}{56} \cdot \frac{2 A_s f_{yd}}{d} \qquad (4)$$

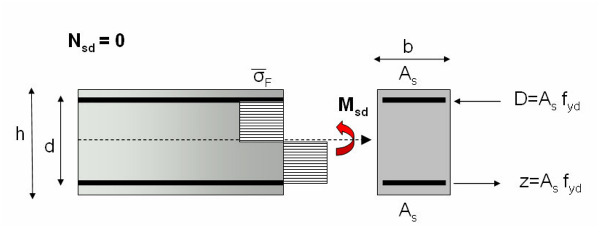

Fig. 4: Pure bending without axial force (N=0)

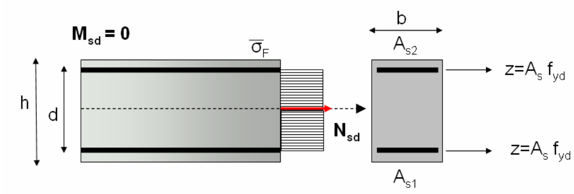

Fig. 5: Pure tension without bending (M=0)

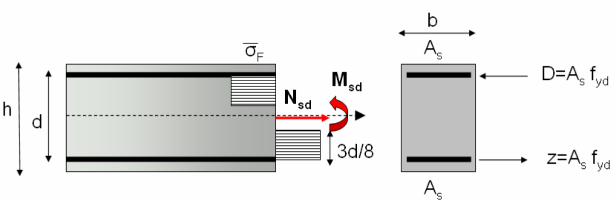

Fig. 6: Uniaxial Bending - Tension (e =M/N=0.93)

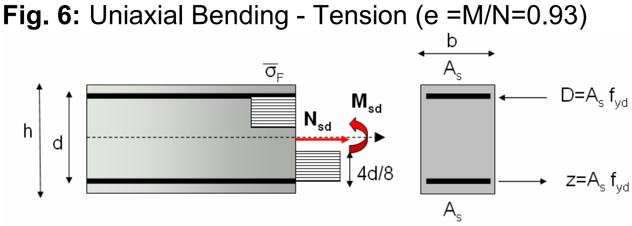

Fig. 7: Uniaxial Bending - Tension (e =M/N=0.33)

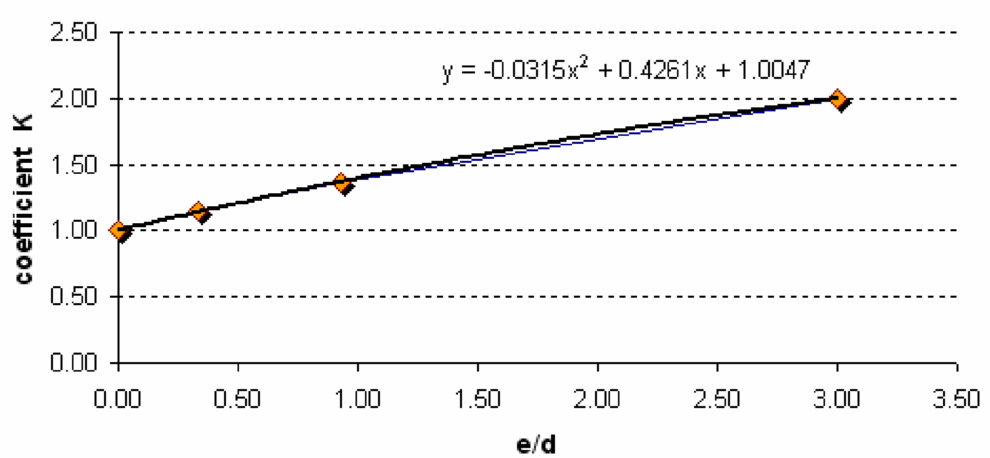

Fig. 8: Coefficient K as a function of section eccentricity

From the above set of equations it is shown that independently of the magnitude of the axial load imposed on a R/C section, the stresses developed are laying within the range of $1x(2A_sf_{yd}/d)$ and $2x(2A_sf_{yd}/d)$ for the extreme cases of N=0 and M=0 respectively, while for the general case, σ_F can be expressed as:

$$\sigma_F = k \times (2A_sf_{yd}/d) \quad (5)$$

Consequently, the variation of the corresponding ration with the eccentricity e/d=M/Nd can be expressed by the following polynomial relationship:

$$K = -0.0315(e/d)^2 + 0.4261(e/d) + 1.0047 \quad (6)$$

Based on the above and the loads anticipated to be applied on the tank bottom, for the particular analysis, the coefficient k can be taken equal to 1.7. As a result, the yielding stress required for the determination of the Von-Mises criterion can be written as:

$$\sigma_F = \frac{2 f_{yd} A_s}{d} \cdot 1.70 \quad (7)$$

Zones of distinct inelastic behaviour

Depending on the existing reinforcement, four zones are distinguished of different flexural strength and section depth for which the corresponding sress-strain relationships are illustrated in Fig. 9. The zone-dependent material properties are illustrated in Table 1 were the required values of yield stress and cohesion are calculated. It is noted that as 'critical zone' of the tank perimeter wall, is defined the first meter at the base of the wall while the 'critical bottom zone' is located at a distance of 2m from the cylinder walls.

Evaluation of the response

Of particular is the non-linear behaviour of the tank for the case that the waste level is diminished starting from the initial level (i.e. +6.80m) given the water table at the level of +3.70m. It is notable that the inelastic analysis was first performed on the assumption that the uplift loads are developed on the undeformed structure (i.e. based on the the tank bottom initial geometry). As a result, it was assumed that the uplift loads were not affected by the dilatation of the bottom slab. It is clear that this is a conservative approach since it is apparent that the more the tank bottom deforms the more less the uplift load is increased. In order to account for the important aspect of this additional geometrical non-linearity, the actual amplitude and distribution of the uplift load was derived.

It is shown in Figure 10 that the system is self-balanced at a fraction (85%) of the load that would have been developed if the tank bottom remained completely undeformed during the tank evacuation. It is very interesting that this is essentially the average fraction of the load because the deformation pattern along the tank radius is non-uniform, hence, the 'relief' is not constant along the tank bottom. Figure 11 also illustrates that the first yielding is observed at the bottom-wall joint when the waste level has been reduced to the level of 1.44m. Based on the above calculations it is concluded that:

- the resulting maximum vertical displacement of the tank bottom is found equal to 0.78m and is in close agreement with the actually measured vertical deflection (0.89m) as described in the previous sections. The deformation shape also matches very well the observed damage pattern.
- the maximum numerically derived strain is equal to 6-10.5‰ (well below the 20‰ threshold defined by the Greek Reinforced Concrete Code ΕΚΟΣ 2000) while the average stress is of the order of 1-3‰, thus in good agreement with the analytical (damage based) prediction of 2.5-4‰.
- the ring pattern of the strain distribution (i.e. ε_x along the y-y axis) calculated equal to 1-3‰ in the region between the central tower and the perimeter walls are compatible with the strain pattern measured on site (Fig. 12).
- the stresses developed at the tank bottom do not lead to the crushing of the concrete even during the time of the complete evacuation of the tank (Fig.13) supporting the argument that the system was essentially self-balanced and did not collapse.

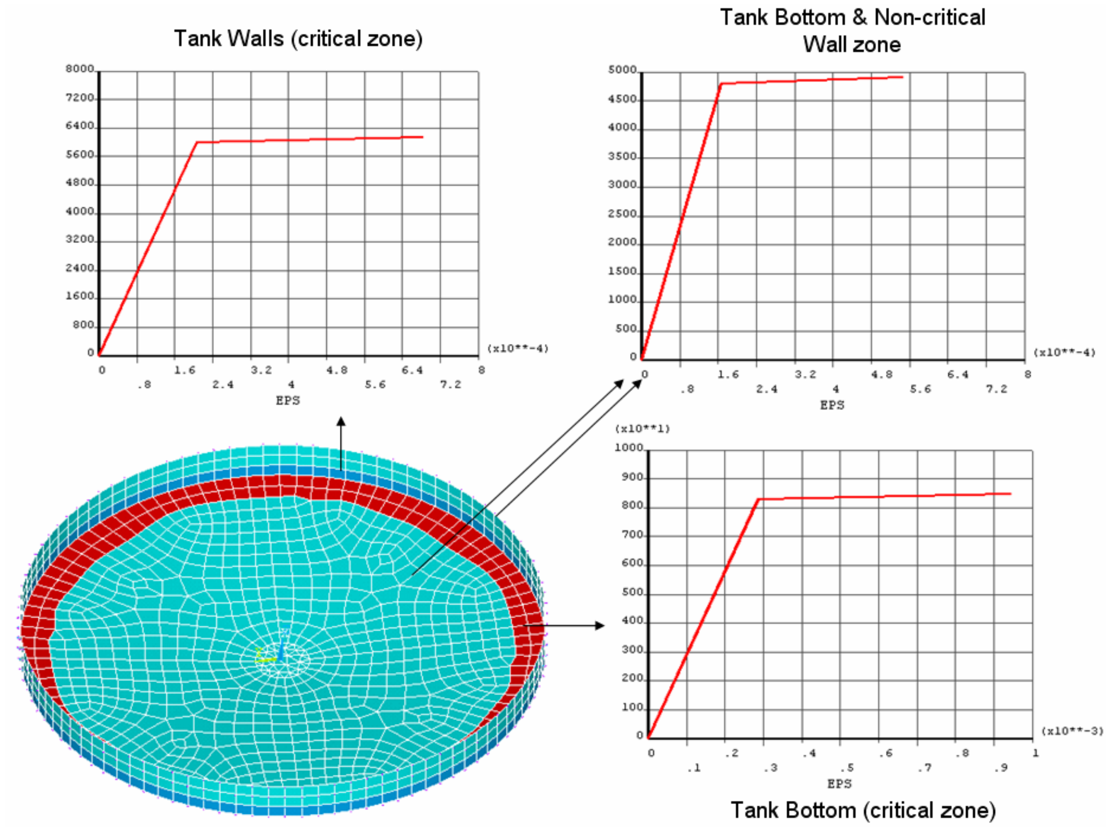

Fig. 9: Material laws for distinct tank zones

Table 1: Analytical determination of the zone-dependent material properties

Zone	Reinforced	Steel	Reinforced (cm^2)	Section Height	Yield stress σy	Cohesion c
Botton (non-critical zone)	#Φ12/90	S500s	12.56 cm^2/m	0.38m	4877 kPa	3980 kPa
Bottom (critical zone)	3.8Φ18/m 3.8Φ16/m 3.8Φ12/m	S500s	21.60 cm^2/m	0.45m	8380 kPa	6800 kPa
Wall (non-critical zone)	#Φ14/100	S500s	15.40 cm^2/m	0.50m	5050 kPa	4090 kPa
Wall (non-critical zone)	#Φ14/85	S500s	18.11 cm^2/m	0.50m	5940 kPa	4810 kPa

Table 2: Compression-only stiffness properties of the uni-axial springs

ZONE	REINFORCEMENT
Tank radius R	27.0m
Embedment depth D	6.0m
Modulus of elasticity of the soil E_s	13.0 MPa
Poisson Ratio	0.3
Shear Modulus G of soil	33.8 MPa
Unit weight γ	19 kN/m^3
Shear wave velocity V_s	130m/sec
Total Vertical stiffness kz	$6.2x10^6$ kN/m
Single spring vertical stiffness	7290 kN/m
Passive pressure $\sigma_p = \gamma K_p z$	57z
Passive pressure coefficient $K_p = 1/K_A$	3
Horizontal stiffness of springs attached at the perimeter walls (as a function of depth z)	162.4 z kN/m

RETROFITTING SCHEME

Based on the above observations and conclusions the retrofitting strategy was formulated on the following two decisions.

(a) The restoration of the capacity of the tanks would be designed to the level defined by the initial design, which corresponds to a water table level of +2,00m, ensuring the preservation of those conditions using a permanent draining and pumping network.

(b) The solid connection of the bottom slab and the perimeter wall has been preserved, leading to the conclusion that an undamaged compression zone is available for future loading.

Description

The basic interventions can be summarized in the following:

(a) Sealing of all the large cracks using epoxy resign from the interior of the tanks

(b) Cathodic protection of the reinforcement

(c) Injection of grout with corrosion inhibitor mixtures in order to further protect the reinforcement, using a 2.00m x2.00m grid.

(d) Construction of a new R/C bottom slab (interior jacket) with a depth of 25cm and a new perimeter wall (interior jacket) up to a height of 1,20m with the same depth.

(e) Connection of this new structure to the existing one using dowels of appropriate dimensions (i.e. Φ12-14 /25x25cm)

(f) Water insulation using appropriate plaster

Application

In order to proceed to the implementation of the retrofitting scheme, it is essential to safely empty the damaged tanks. For that the water table at the perimeter has to be decrease to -0.50m in order to achieve a water table level of +1.00m at the center of the tanks. To safely apply this condition the following steps were prescribed:

(i) Evacuation of the tanks up to the water table level of +4.00m

(ii) Decrease of the water table level of 0.50m to the value of 3.50m. Monitoring of the pressumeter readings and the crack width within the tanks

(iii) Evacuation of the tanks to the water table level of 3.50m. Monitoring of the pressumeter readings and the crack width within the tanks

(iv) Repetition of the procedure until the desired water table level is reached.

(v) Close monitoring of the tank bottom slab displacements to exclude the possibility of the water table being higher than estimated at the center of the tanks.

CONCLUSION

In this paper, the analytical approaches selected in order to assess the conditions of the two underground tanks which were damaged by an unexpected increase of the geotechnical parameters (water table level) were presented. More specifically, the non visible part of the two tanks (bottom of the foundation slab) was assessed using simple yet sophisticated hand calculations, which incorporated the filed observations such as deformations and total crack width, and a set of complex nonlinear analysis which produced results in close agreement. The conclusion that the bottom surface of the tank had not suffered concrete crushing due to compression was safely derived and therefore retrofitting was performed as the optimum solution.

REFERENCES

ANSYS Inc. (2002) *'ANSYS User's Manual, Version 8.1'*, Canonsburg, PA.

ANSYS Inc. (2004) *'ANSYS Programmers Guide',* Canonsburg, PA.

Kappos, A. & Sextos, A. (2001) 'Effect of foundation type and compliance on the lateral load response of R/C bridges', Jrl of Bridge Eng, ASCE., Vol. 6, 120-130.

Mylonakis, G. Gazetas, G.. Nikolaou, S. and Chauncey, A. (2003) 'Development of analysis and design procedures for spread footings', MCEER, *State University of New York at Buffalo*, Report No. 02-0003.

Ministry of Public Works (2000) 'Hellenic Code for Reinforced Concrete', Athens (in Greek)

Penelis G, & Kappos A.(1997), '*Earthquake Resistant Concrete Structures',* E& FN SPON, London

Sextos (2005) 'A computer interface for importing refined spatially variable earthquake ground motions into 3D models developed with ANSYS', 23. CADFEM Users´ Meeting International Congress on FEM Technology with ANSYS CFX & ICEM CFD Conference, Berlin (accepted for publication).

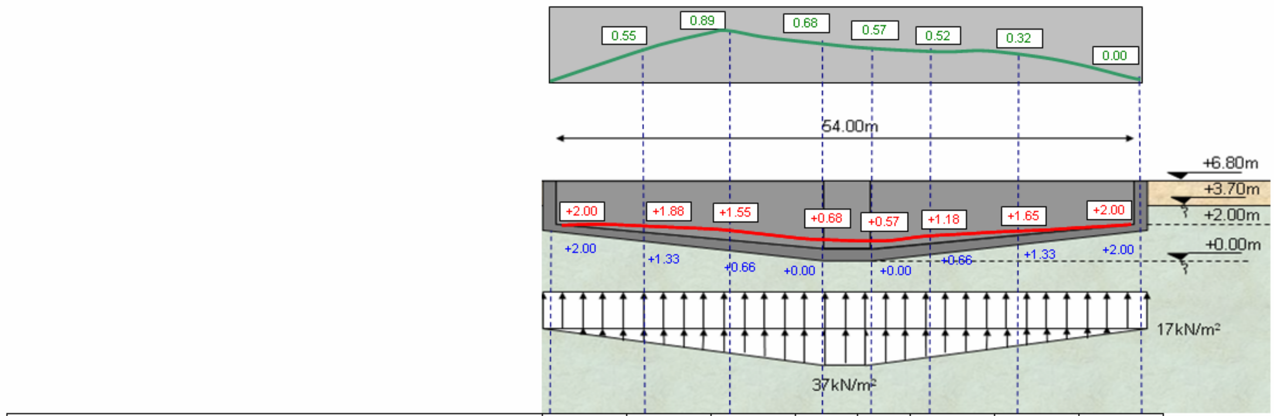

Initial Coordinates of the undeformed shape (z)	2.00	1.33	0.66	0.00	0.00	0.66	1.33	2.00
Measured Uplift δ	0.00	0.55	0.89	0.68	0.57	0.52	0.32	0.00
Deformed Structure Level Uz = z + δ	2.00	1.88	1.55	0.68	0.57	1.18	1.65	2.00
ΔH of actual uplift = 3.70 - z - δ	1.70	1.82	2.15	3.02	3.13	2.52	2.05	1.70
Uplift (kPa) = ΔH * 10	17.00	18.21	21.47	30.19	31.27	25.22	20.54	17.00
Calculated ΔH' (uplift on the undeformed tank) = 3.70 - z	1.70	2.37	3.04	3.70	3.70	3.04	2.37	1.70
Calculated uplift load on the undeformed tank (kPa) = ΔH' * 10	17.00	23.70	30.40	37.00	37.00	30.40	23.70	17.00
% of the calculated load of the inelastic analysis corresponding to the observed and measured bottom deflection	100%	77%	71%	82%	85%	83%	87%	100%
Average Load (%)	85%							

Fig.10: Determination of the average fraction of the (elastically calculated) hydrostatic pressure for which the system equilibrates

load %	Waste level (m)	ΔH (m)	max U_z (cm)
	6.00	-2.30	-0.49
0	3.70	0.00	0
51.4%	2.00	1.70	5.9
61.1%	1.44	2.26	8.5
67.6%	1.20	2.50	14.2
85.0%	0.89	2.81	78.1
100.0%	0.00	3.70	177.2

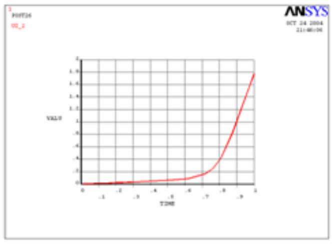

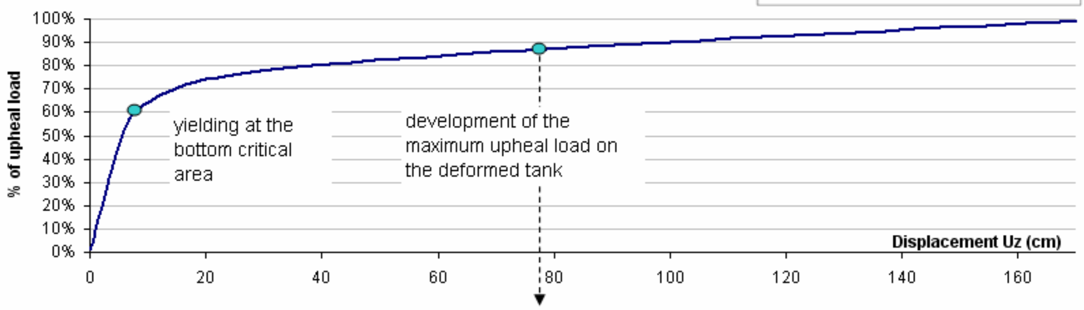

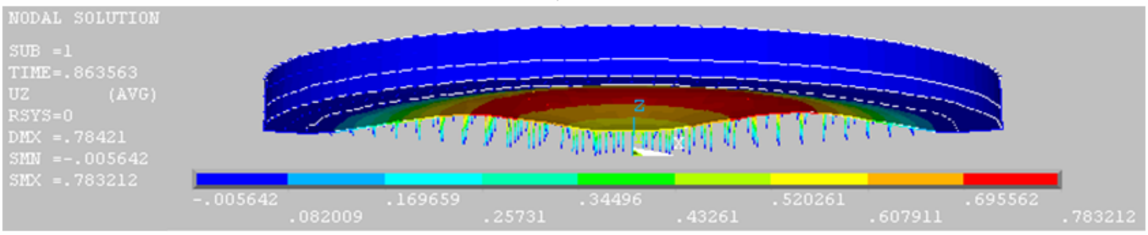

Fig. 11: Variation of the maximum bottom vertical displacement with the load build-up attributed to the gradual evacuation of the tank

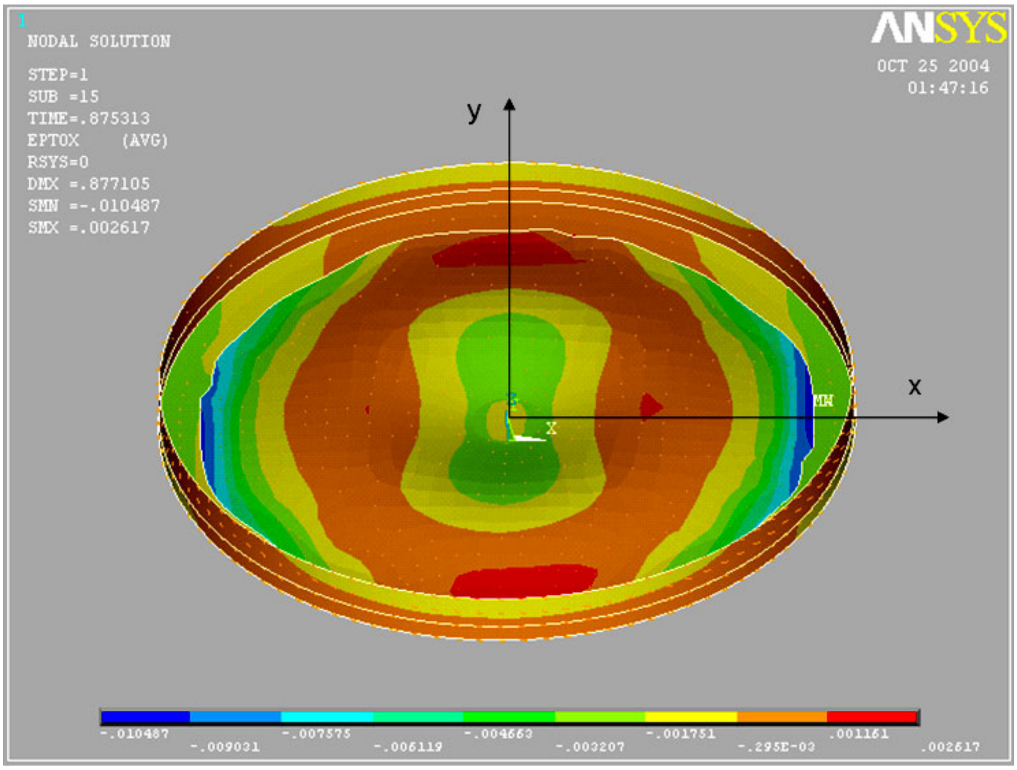

Fig. 12: Strain distribution at the time that the system equilibrates

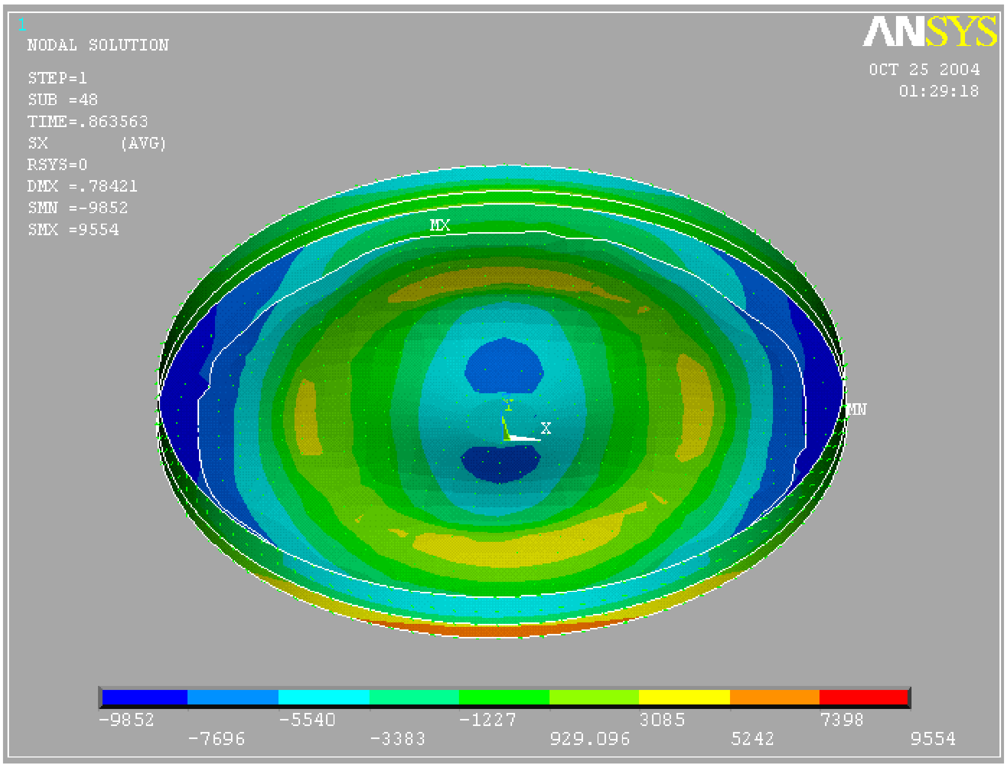

Fig. 13: Normal stress (σ_{xx}) distribution at the time that the system equilibrates (KPa)